

Published in final edited form as:

Arterioscler Thromb Vasc Biol. 2013 March ; 33(3): 481–488. doi:10.1161/ATVBAHA.112.255737.

Dynamin-related protein-1 controls fusion pore dynamics during platelet granule exocytosis

Secil Koseoglu², James R. Dilks¹, Christian G. Peters¹, Jennifer L. Fitch¹, Nathalie A. Fadel¹, Reema Jasuja¹, Joseph E. Italiano Jr.^{3,4}, Christy L. Haynes², and Robert Flaumenhaft¹

¹Division of Hemostasis and Thrombosis, Department of Medicine, BIDMC, Harvard Medical School, Boston, MA

²Department of Chemistry, University of Minnesota, Minneapolis, MN

³Division of Hematology, Department of Medicine, Brigham and Women's Hospital, Boston, MA

⁴Vascular Biology Program, Department of Surgery, Children's Hospital, Boston, MA

Abstract

Objective—Platelet granule exocytosis serves a central role in hemostasis and thrombosis. Recently, single-cell amperometry has shown that platelet membrane fusion during granule exocytosis results in the formation of a fusion pore that subsequently expands to enable the extrusion of granule contents. However, the molecular mechanisms that control platelet fusion pore expansion and collapse are not known.

Methods and Results—We identified dynamin-related protein 1 (Drp1) in platelets and found that an inhibitor of Drp1, mdivi-1, blocked exocytosis of both platelet dense and α -granules. We used single-cell amperometry to monitor serotonin release from individual dense granules and thereby measured the effect of Drp1 inhibition on fusion pore dynamics. Inhibition of Drp1 increased spike width and decreased pre-spike foot events, indicating that Drp1 influences fusion pore formation and expansion. Platelet-mediated thrombus formation *in vivo* following laser-induced injury of mouse cremaster arterioles was impaired following infusion of mdivi-1.

Conclusions—These results demonstrate that inhibition of Drp1 disrupts platelet fusion pore dynamics and indicate that Drp1 can be targeted to control thrombus formation *in vivo*.

Keywords

platelets; exocytosis; dynamin-related protein-1; fusion pore; thrombosis

Introduction

Platelet granules are required for normal hemostasis and contribute to pathological thrombus formation. Platelet granule exocytosis has also been implicated in numerous other physiological functions, including inflammation, microbial host defense, angiogenesis, and wound healing. Platelet granule types include α -granules (50–80 granules/platelet), dense granules (3–6 granules/platelet), and lysosomes (0–3 granules/platelet). These granules release their contents following stimulation of receptors on the platelet surface. Although

Address correspondence to: Robert Flaumenhaft, M.D., Ph.D., Center for Life Science, Rm 939, Beth Israel Deaconess Medical Center, 3 Blackfan Circle, Boston, MA, 02215., Tel: 617-735-4005, Fax: 617-735-4000, rflaumen@bidmc.harvard.edu.

Conflict of Interest Disclosure

The authors have no conflict of interest to declare.

much has been learnt about the proximal signal transduction mechanisms that mediate the release of granule contents following stimulation of surface receptors, considerably less is known about the distal mechanisms that facilitate granule exocytosis.

Exocytosis of platelet granule contents requires the fusion of granule membranes with plasma membranes or membranes of the open canalicular system.¹ The release of contents likely occurs through a dynamic fusion pore. Electrophysiological techniques have been used to study the formation, expansion, and collapse of the fusion pore in neurons and neuroendocrine cells. Yet the mechanisms regulating the platelet fusion pore are poorly understood, and the proteins that control platelet fusion pore dynamics have not been identified. Platelet fusion pore dynamics have been difficult to study by standard electrophysiological methods because of their small size and atypical membrane system. Single-cell amperometry, however, has sufficient temporal and spatial resolution to evaluate fusion pore dynamics in live platelets and has recently been used to study quantal release of serotonin from individual dense granules.²⁻⁵ Amperometric tracings of platelet dense granule release demonstrate features previously observed only in nucleated cells, indicating that stable fusion pore formation, fusion pore expansion, and 'kiss-and-run' exocytosis occur in platelets. We have previously used amperometry of individual platelets to evaluate mechanisms of platelet membrane pore dynamics.²⁻⁶

We now use single-cell amperometry to study the role of dynamin-related protein 1 (Drp1) in platelet granule release. Drp1 belongs to the dynamin superfamily, a group of large GTPases that act as mechanoenzymes and demonstrate oligomerization-dependent GTPase as well as membrane modeling activities.⁷ Drp1 is most widely known for its role in mediating mitochondrial fission and fusion. We demonstrate that platelets contain Drp1 and that Drp1 is phosphorylated upon platelet activation. Blocking Drp1 inhibits platelet granule exocytosis and impairs fusion pore stability. Inhibition of Drp1 also interferes with platelet accumulation during thrombus formation *in vivo*. These studies demonstrate a heretofore unrecognized function of Drp1 in platelet physiology.

Methods

Platelet preparation

Human and rabbit platelets were prepared as described in the supplementary methods (please see <http://atvb.ahajournals.org>).

Single-cell amperometry

Amperometry experiments were performed with an Axopatch 200B potentiostat (Molecular Devices, Inc.) controlled by locally written LABVIEW software. Fabrication of carbon-fiber microelectrodes and the experimental instrumentation have been previously described.^{2, 4, 8} Rabbit platelets were used for these experiments because they have a substantially higher number of dense granules per platelet than human platelets. To begin a measurement, a drop of rabbit platelet suspension was added to the experimental chamber that contained either 10 μ M mdivi-1 (Tocris), or 10 μ M compound E (generous gift of Dr. Jodi Nunnari and Dr. Ann Cassidy-Stone) in Tyrode's buffer (prepared from stock solutions in DMSO) or the same volume of DMSO in Tyrode's buffer for experimental and control conditions, respectively. Platelets were allowed to sediment on poly L-lysine-coated coverslips for 15 minutes before amperometry measurements. One platelet at a time was stimulated with a 3 s bolus of thrombin solution in Tyrode's buffer (10 U/mL), and the amperometric response was recorded for 60 s. Data were analyzed as has been previously described⁴ and reported as mean \pm SEM; t-tests were used to identify statistically significant differences compared to the

control condition. Amperometric measurements were recorded from 107 platelets for control condition, 39 platelets for mdivi-1 condition, and 31 platelets for the compound E condition.

Thrombus formation model

Intravital video microscopy of the cremaster muscle microcirculation was performed as previously described.⁹ Mouse anti-human fibrin II β -chain monoclonal antibody was purified over protein G-Sepharose (Invitrogen) from a 59D8 hybridoma cell line¹⁰ and labeled with Alexa Fluor 488 (Invitrogen). Digital images were captured with a Cooke Sensicam CCD camera (The Cooke Corporation) connected to a VS4-1845 Image Intensifier GEN III (Video Scope International). Injury to a cremaster arteriolar (30–50 μ m diameter) vessel wall was induced with a Micropoint Laser System (Photonics Instruments) focused through the microscope objective, parfocal with the focal plane and tuned to 440 nm through the dye cell containing 5 mM coumarin in methanol. Data were captured digitally from two fluorescence channels, 488/520 nm and 647/670 nm. Data acquisition was initiated both prior to and following a single laser pulse for each injury. The microscope system was controlled and images were analyzed using Slidebook (Intelligent Imaging Innovations).

Image analysis

For each thrombus generated, a rectangular mask was defined that included a portion of the vessel upstream of the site of injury. The maximum fluorescence intensity of the pixels contained in this mask was extracted for all frames (pre- and post-injury) for each thrombus. The mean value calculated from the maximal intensity values in the mask for each frame was determined and used as the background value. Finally, for each frame the integrated fluorescence intensity was calculated as per following equation:

$$\text{Integrated fluorescence intensity} = \text{sum intensity of signal} - (\text{mean of the maximal background intensity} \times \text{area of the signal}).$$

This calculation was performed for all frames in each thrombus and plotted versus time to provide the kinetics of thrombus formation. For multiple fluorescence channels, calculations of background were made independently for each channel. The data from 25–30 thrombi were used to determine the median value of the integrated fluorescence intensity to account for the variability of thrombus formation at any given set of experimental conditions.

Statistical analysis

A value representing area under the curve was calculated for each curve generated by measurement of fluorescence following laser injury of an arteriole. A Mann-Whitney test was used for statistical comparison of data sets comprised of the indicated number of thrombi formed under each indicated condition. *P* values of 0.05 or less were considered statistically significant and are indicated. Statistical analyses were performed using Prism software package (version 4; GraphPad).

Immunoblot analysis

Immunoblot analysis of human platelet lysates was performed as described in the supplementary methods.

Immunogold Electron and Immunofluorescence Microscopy

Human platelets were analyzed using transmission electron microscopy and immunofluorescence microscopy as described in the supplementary methods.

Flow cytometry

Flow cytometry was used to quantify P-selectin surface exposure to monitor α -granule release and measure JC-1 fluorescence to monitor mitochondrial membrane potential as described in the supplementary methods.

Detection of adenine nucleotide release

A luciferin-luciferase detection system was used to measure ADP/ATP release to monitor dense granule secretion as described in the supplementary methods.

Results

Dynamins in platelets

Dynamins are a superfamily of large GTPases that serve a wide range of membrane shaping functions.⁷ Their expression and function in platelets is not well-understood. Megakaryocytes have previously been shown to express dynamin 3.^{11, 12} However, whether other dynamins and dynamin-related proteins are present in platelets has not been assessed. We therefore evaluated platelet lysates for dynamin 1, dynamin 2, and Drp1. Dynamin 1 was not identified under the conditions of our assay. In contrast, dynamin 2 and Drp1 were recognized as single bands with apparent molecular weights of 100 kD and 80 kD, respectively (Fig. 1A). No additional bands were detected in immunoblots of platelet lysates. To evaluate for the presence of Drp1 in platelet cytosol, platelets were permeabilized with streptolysin-O and subsequently pelleted. Evaluation of platelet cytosol and membranes demonstrated Drp1 in both fractions (Fig. 1B), indicating that a portion of platelet Drp1 is cytosolic. Evaluation of activation-dependent phosphorylation of platelet Drp1 using phosphorylation site specific antibodies demonstrated that Drp1 is phosphorylated at serine 616 following incubation with SFLLRN to activate PAR1 and at serine 637 following incubation with forskolin to activate adenylyl cyclase (Fig. 1C). Immunogold electron microscopy was performed to further define the localization of Drp1 in platelets. Electron microscopy demonstrated that Drp1 associated with granule membranes and the cytoplasmic face of the platelet plasma membrane and was present in the cytosol (Fig. 1E; supplementary fig. I; please see <http://atvb.ahajournals.org>). Studies using a non-immune antibody demonstrated no staining (supplementary fig. I). These results show that Drp1 is found in platelets, is phosphorylated in an activation-dependent manner, and localizes to both membranes and cytosol.

Drp1 functions in platelet granule exocytosis

Dynamins have a well-established role in endocytosis,^{7, 13, 14} associating with the stalk of the maturing endocytotic vesicle and catalyzing vesicle scission. More recently, dynamins have been shown to function in granule exocytosis.¹⁵⁻²⁰ To evaluate whether dynamins function in platelet granule exocytosis, we tested the effect of the dynamin inhibitors, dynasore and MiTMAB, on exocytosis using surface expression of P-selectin as a marker of α -granule release (Fig. 2). Dynasore blocked agonist-induced P-selectin surface expression with an IC_{50} of approximately $20 \mu M_{21}$ (Fig. 2), close to its IC_{50} for recombinant dynamin in a GTPase assay. MiTMAB also inhibited P-selectin surface expression with an IC_{50} of approximately $20 \mu M$ (Fig. 2). These results indicate a role for dynamins in platelet granule exocytosis. Dynasore and MiTMAB have been used widely to assess the role of dynamin family proteins in cell function.^{21, 22} However, they are general inhibitors of dynamins and cannot be used to assess the role of specific dynamin subtypes in exocytosis.

Drp1 is widely known for its role in mitochondrial fission²³⁻²⁷ and fusion.²⁸ However, a role in degranulation has also been described.²⁹ To determine whether Drp1 functions in platelet granule exocytosis, we used the well-characterized Drp1 inhibitor, mitochondrial

division inhibitor-1 (mdivi-1). Mdivi-1 selectively blocks Drp1, but not other dynamin isoforms, and acts outside of the GTP binding site.³⁰ This inhibitor blocked PAR1-mediated α -granule release with an IC₅₀ of approximately 10 μ M (Fig. 3A), similar to its IC₅₀ for inhibition of recombinant Drp1 in a GTPase assay.³⁰ One method to assess the selectivity of a small molecule for a particular protein target is to use compound analogs that vary in their ability to inhibit the target and determine whether or not their activity is replicated in the cellular system of interest. Analogs of mdivi-1 were used to assess whether Drp1 is the relevant target of mdivi-1 in platelet granule exocytosis. Compound D, an analog with potency equal to that of mdivi-1 against recombinant Drp1 in a GTPase assay,³⁰ demonstrated similar potency to mdivi-1 in an assay of α -granule release (Fig. 3A). Compound E was substantially less potent than mdivi-1 against recombinant Drp1 in a GTPase assay, demonstrating only approximately 45% inhibition at 50 μ M.³⁰ Therefore, if Drp-1 is the relevant target for mdivi-1 in platelet exocytosis, then compound E would demonstrate significantly less activity than mdivi-1 in the secretion assay. Compound E was significantly less active in inhibiting platelet α -granule release (Fig. 3A). To determine whether Drp1 functions in dense granule release as well as α -granule release, we evaluated the role of mdivi-1 on adenine nucleoside release using a luciferase-based assay. Dense granule release was inhibited by mdivi-1 with an IC₅₀ of approximately 10 μ M (Fig. 3B). These results indicate a role for Drp1 in platelet granule exocytosis.

Drp1 controls platelet fusion pore dynamics

Drp1 functions in mitochondrial dynamics that contribute to granule secretion in mast cell exocytosis, synapses, and insulin-secreting cells.^{29, 31, 32} We used single-cell amperometry to evaluate, with sub-millisecond resolution, the effect of mdivi-1 on the release of serotonin from rabbit platelets (Fig. 4A). Statistical analyses of multiple tracings showed that 10 μ M mdivi-1 had no effect on the quantal concentration of released serotonin (Fig. 4B) or the number of fusion events per platelet (Fig. 4C), which enabled unambiguous evaluation of the change in fusion pore behavior and kinetics of release. Results showed that although 10 μ M mdivi-1 did not affect the time required for transition from fusion pore to maximal release (T_{rise}) (Fig. 4D), it changed the kinetics of the total release event (Fig. 4E). The prolonged spike width in amperometric tracings from platelets exposed to mdivi-1 indicated that mdivi-1 reduced the efficiency of serotonin release through the fusion pore. Time of half maximal release ($T_{1/2}$) was 14.97 ± 0.81 ms for control and 23.00 ± 1.70 ms for mdivi-1 conditions (Fig. 4E). This effect can be observed in figure 4A (see inset), where representative spikes for each condition are shown above the tracings; mdivi-1 treated cells produced wider (larger $T_{1/2}$) and smaller amplitude spikes (since the Q values are similar) upon release of serotonin. Amplitude analysis demonstrated a mean amplitude of 16.58 ± 1.35 pA in control samples compared with 8.96 ± 0.93 pA in samples incubated with mdivi-1 ($p=0.0004$). In contrast, compound E had no effect on spike amplitude or $T_{1/2}$ (supplementary fig. II). This result demonstrates that mdivi-1 impairs efficient extrusion of serotonin from platelet dense granules.

Additional characteristics of amperometric tracings were evaluated to assess the role of Drp1 on the rate of dense granule release and on fusion pore stability (Fig. 5). Cumulative frequency analyses indicate how efficiently granules are trafficked, docked, and fuse upon stimulation.⁶ Since the percent of granules released over time does not change upon mdivi-1 treatment (Fig. 5B), it is unlikely that mdivi-1 influences delivery of granules to surface connected membranes by cytoskeletal transport or docking at the release site. Following membrane fusion and initial pore formation, pore expansion can ensue, leading to full granule collapse and concomitant extrusion of granule contents. Initial formation of the fusion pore can be identified in amperometric spikes as a subtle increase in the current which is called a 'foot'. Alternatively, the fusion pore can close after partial secretion in an

event termed kiss-and-run exocytosis (Fig. 5A). In this work, standalone spikes with an integrated area between 30 fC (approximately 100 times the RMS noise of each tracings) and 100 fC (approximately 30% of the average Q value) are classified as kiss and run events. Release events through fusion pores followed by either reclosure of the fusion pore or full release following foot process formation were monitored. The total %kiss-and-run events did not differ significantly between the two conditions (Fig. 5C). However, there was a significant difference between the fusion events completed by full fusion through a foot process in control platelets versus platelets exposed to mdivi-1 (Fig. 5D) (% foot is 17.35 ± 1.37 for control and 9.46 ± 2.01 for mdivi-1 conditions, $p < 0.01$). In contrast to the effects of mdivi-1, compound E had no effect on platelet pore formation (supplementary fig. II). These results indicate that inhibition of Drp1 impairs fusion pore stability.

Drp1 antagonism inhibits thrombus formation

Inhibition of Drp1 following infusion of mdivi-1 has previously been demonstrated to block reperfusion injury in cardiac, renal and retinal ischemia models.^{33–35} The protective effect has been attributed to prevention of mitochondrial fragmentation since Drp1 is known to function in mitochondrial fission.^{26, 27} However, antiplatelet compounds can also confer protection against reperfusion injury, and platelet function was not evaluated in previous studies. Since inhibition of Drp1 inhibits platelet exocytosis, we determined whether pharmacological inhibition of Drp1 could control thrombus formation following vascular injury. Platelet accumulation (Fig. 6A, *red*) and fibrin formation (Fig. 6A, *green*) were monitored following laser-induced injury of cremaster arterioles prior to (Fig. 6A; supplementary video S1) and following infusion of mdivi-1 (Fig. 6B; supplementary video S2). A 59% reduction in platelet accumulation ($p < 0.001$, as determined by AUC) was observed following infusion of mdivi-1 (Fig. 6C, supplementary fig. III). In contrast, there was no significant effect of mdivi-1 on fibrin generation following laser-induced vascular injury (Fig. 6D, supplementary fig. III), consistent with other interventions specifically targeting platelet function in this model.³⁶

Discussion

These experiments evaluate the role of Drp1 in platelet function using small molecules. The indication that Drp1 functions in granule exocytosis was originally derived from a chemical genetic screen of $>300,000$ compounds to identify inhibitors of platelet granule secretion.³⁷ This unbiased forward screen identified a compound, ML160, which also demonstrated activity in an assay designed to identify inhibitors of the product of yeast *Dnm1*, the yeast ortholog of Drp1. Following the identification of ML160 as an inhibitor of platelet exocytosis, we used two well-characterized dynamin family inhibitors, dynasore and MiTMAB, which also blocked platelet granule secretion (Fig. 2). This result implicates dynamin family proteins in platelet granule release. To evaluate the role of Drp1 in granule release, we used mdivi-1, which is selective for Drp1 and has proven to be a useful compound in its study.^{30, 34, 35, 38, 39} Mdivi-1 inhibits exocytosis in the same concentration range that it inhibits the recombinant Drp1 GTPase activity. The fact that the inhibitory activity of various mdivi-1 analogs in the exocytosis assay mirror their activity against the recombinant Drp1 GTPase (Fig. 3) further supports the premise that Drp1 is the relevant target of mdivi-1 in the exocytosis assay.

Studies demonstrating a role for Drp1 in granule secretion^{29, 31, 32} prompted us to evaluate the effect of mdivi-1 on serotonin release from individual granules using single-cell amperometry. Experiments were conducted with a low concentration of mdivi-1 ($10 \mu\text{M}$) so as not to impair total quantal release of serotonin [Q(fC)] and to enable direct comparison of tracings with untreated controls. Lower antagonist concentrations also decrease the likelihood of off-target effects. These studies demonstrated that mdivi-1 has a significant

effect on spike width and the percent of foot processes associated with spikes (Figs. 4 and 5). Figure 4 shows representative traces from both control and mdivi-1-exposed platelets. Unlike the control platelets, mdivi-1-treated platelets show an extended release behavior for each fused granule. This result implies that mdivi-1 impairs the rate of expansion of the fusion pore, and thus, slows the time course for serotonin release from individual granules. Moreover, foot process formation was inefficient when platelets were exposed to mdivi-1, demonstrating that inhibition of Drp1 causes fusion pore instability.

There are several potential mechanisms by which Drp1 may control fusion pore dynamics. Drp1 colocalizes with mitochondria in platelets (supplementary fig. IV) and could participate in granule secretion via effects on mitochondria. In mast cells, either incubation with mdivi-1 or treatment with Drp1 siRNA blocks mitochondrial translocation required for activation-induced TNF- α and β -hexoseaminidase release.²⁹ Mitochondria play a prominent role in insulin secretion by generating required ATP and metabolites that stimulate secretory processes.⁴⁰ Silencing Drp1 impairs insulin secretion in the hypothalamus.³² Mitochondria also contribute to synaptic vesicle release⁴¹ and Drp1 has been shown to function in this capacity.³¹ Mdivi-1 impairs mitochondrial permeability transition pore (MPTP) formation and reduces ischemia mediated death in cardiomyocytes.³³ However, under the conditions of our assay, we found no effect of mdivi-1 on mitochondrial membrane potential (supplementary fig. V). Similarly, mdivi-1 had no effect on platelet apoptosis as measured by annexin V binding (data not shown). In contrast, antimycin A, an inhibitor of mitochondrial respiration, impaired mitochondrial membrane potential without blocking granule secretion (supplementary fig. V). Thus, impairment of mitochondrial membrane potential is not a likely explanation for the effects of mdivi-1 on granule secretion. An alternative possibility is that Drp1 acts to control fusion pore formation at the site of stalk formation. Unlike classical dynamins, Drp1 lacks a pleckstrin homology domain or SH3 domain and is not known to act at sites of membrane fusion. Nonetheless, Drp1 interacts with membranes and could potentially influence pore expansion directly. Further studies will be required to determine the mechanism by which Drp1 controls platelet fusion pore dynamics.

Inhibition of Drp1 blocked platelet accumulation during thrombus formation following vascular injury. In contrast, fibrin generation was unaffected (Fig. 6). This observation is consistent with the fact that fibrin generation following laser-induced injury of the cremaster arteriole is independent of platelet accumulation.³⁶ Infusion of mdivi-1 has previously been shown to decrease infarct size in murine ventricles in an *in vivo* model of cardiac ischemia-reperfusion injury.³³ Systemic infusion of 50 mg/kg of mdivi-1 has also been used to reverse ischemic renal injury and tubular apoptosis induced by reperfusion following renal ischemia.³⁴ The effect was attributed to suppression of ischemia-induced mitochondrial fragmentation. Similarly, mdivi-1 was shown to inhibit early neurodegenerative events and increase retinal ganglion cell survival following acute retinal ischemia.³⁵ Our results using the same mdivi-1 concentration demonstrate that mdivi-1 is an antiplatelet agent in the setting of injury-induced thrombus formation. A limitation of our studies is that we cannot restrict the activity of mdivi-1 to platelets following systemic infusion. We cannot rule out an effect of mdivi-1 on endothelial cells or leukocytes in our assay. Nonetheless, since antiplatelet therapy can prevent tissue damage following reperfusion⁴²⁻⁴⁴ and mdivi-1 interferes with platelet secretion, effects on platelet function must also be considered when assessing the role of Drp1 in reperfusion injury. The combination of maintaining vascular patency and inhibiting apoptosis may be useful in the treatment of ischemic injury.

Supplementary Material

Refer to Web version on PubMed Central for supplementary material.

Acknowledgments

This work was supported by NIH grant HL87203 (R.F.) and NIH New Innovator Award to C. L. H (OD004258-01). R.F. is a recipient of an Established Investigator Award from the American Heart Association (0840043N).

References

1. Blair P, Flaumenhaft R. Platelet alpha-granules: basic biology and clinical correlates. *Blood Rev.* 2009; 23:177–189. [PubMed: 19450911]
2. Ge S, Wittenberg NJ, Haynes CL. Quantitative and real-time detection of secretion of chemical messengers from individual platelets. *Biochemistry.* 2008; 47:7020–7024. [PubMed: 18557631]
3. Ge S, Woo E, White JG, Haynes CL. Electrochemical measurement of endogenous serotonin release from human blood platelets. *Anal Chem.* 2011; 83:2598–2604. [PubMed: 21384903]
4. Ge S, White JG, Haynes CL. Quantal release of serotonin from platelets. *Anal Chem.* 2009; 81:2935–2943. [PubMed: 19364141]
5. Ge S, White JG, Haynes CL. Critical role of membrane cholesterol in exocytosis revealed by single platelet study. *ACS Chem Biol.* 2010; 5:819–828. [PubMed: 20590163]
6. Ge S, White JG, Haynes CL. Cytoskeletal F-actin, not the circumferential coil of microtubules, regulates platelet dense-body granule secretion. *Platelets.* 2011
7. Praefcke GJ, McMahon HT. The dynamin superfamily: universal membrane tubulation and fission molecules? *Nat Rev Mol Cell Biol.* 2004; 5:133–147. [PubMed: 15040446]
8. Wightman RM, Jankowski JA, Kennedy RT, Kawagoe KT, Schroeder TJ, Leszczyszyn DJ, Near JA, Diliberto EJ Jr, Viveros OH. Temporally resolved catecholamine spikes correspond to single vesicle release from individual chromaffin cells. *Proc Natl Acad Sci U S A.* 1991; 88:10754–10758. [PubMed: 1961743]
9. Graham GJ, Ren Q, Dilks JR, Blair P, Whiteheart SW, Flaumenhaft R. Endobrevin/VAMP-8-dependent dense granule release mediates thrombus formation in vivo. *Blood.* 2009; 114:1083–1090. [PubMed: 19395672]
10. Jasuja R, Passam FH, Kennedy DR, Kim SH, van Hessem L, Lin L, Bowley SR, Joshi SS, Dilks JR, Furie B, Furie BC, Flaumenhaft R. Protein disulfide isomerase inhibitors constitute a new class of antithrombotic agents. *J Clin Invest.* 2012; 122:2104–2113. [PubMed: 22565308]
11. Reems JA, Wang W, Tsubata K, Abdurrahman N, Sundell B, Tijssen MR, van der Schoot E, Di Summa F, Patel-Hett S, Italiano J Jr, Gilligan DM. Dynamin 3 participates in the growth and development of megakaryocytes. *Exp Hematol.* 2008; 36:1714–1727. [PubMed: 19007685]
12. Wang W, Gilligan DM, Sun S, Wu X, Reems JA. Distinct Functional Effects for Dynamin 3 During Megakaryocytopoiesis. *Stem Cells Dev.* 2011; 20:2139–2151. [PubMed: 21671749]
13. Verma DP, Hong Z. The ins and outs in membrane dynamics: tubulation and vesiculation. *Trends Plant Sci.* 2005; 10:159–165. [PubMed: 15817416]
14. Ramachandran R. Vesicle scission: dynamin. *Semin Cell Dev Biol.* 2011; 22:10–17. [PubMed: 20837154]
15. Graham ME, O’Callaghan DW, McMahon HT, Burgoyne RD. Dynamin-dependent and dynamin-independent processes contribute to the regulation of single vesicle release kinetics and quantal size. *Proc Natl Acad Sci U S A.* 2002; 99:7124–7129. [PubMed: 11997474]
16. Tsuboi T, McMahon HT, Rutter GA. Mechanisms of dense core vesicle recapture following “kiss and run” (“cavcapture”) exocytosis in insulin-secreting cells. *J Biol Chem.* 2004; 279:47115–47124. [PubMed: 15331588]
17. Fulop T, Doreian B, Smith C. Dynamin I plays dual roles in the activity-dependent shift in exocytic mode in mouse adrenal chromaffin cells. *Arch Biochem Biophys.* 2008; 477:146–154. [PubMed: 18492483]
18. Gonzalez-Jamett AM, Baez-Matus X, Hevia MA, Guerra MJ, Olivares MJ, Martinez AD, Neely A, Cardenas AM. The association of dynamin with synaptophysin regulates quantal size and duration of exocytotic events in chromaffin cells. *J Neurosci.* 2010; 30:10683–10691. [PubMed: 20702699]

19. Anantharam A, Bittner MA, Aikman RL, Stuenkel EL, Schmid SL, Axelrod D, Holz RW. A new role for the dynamin GTPase in the regulation of fusion pore expansion. *Mol Biol Cell*. 2011; 22:1907–1918. [PubMed: 21460182]
20. Anantharam A, Onoa B, Edwards RH, Holz RW, Axelrod D. Localized topological changes of the plasma membrane upon exocytosis visualized by polarized TIRFM. *J Cell Biol*. 2010; 188:415–428. [PubMed: 20142424]
21. Macia E, Ehrlich M, Massol R, Boucrot E, Brunner C, Kirchhausen T. Dynasore, a cell-permeable inhibitor of dynamin. *Dev Cell*. 2006; 10:839–850. [PubMed: 16740485]
22. Quan A, McGeachie AB, Keating DJ, van Dam EM, Rusak J, Chau N, Malladi CS, Chen C, McCluskey A, Cousin MA, Robinson PJ. Myristyl trimethyl ammonium bromide and octadecyl trimethyl ammonium bromide are surface-active small molecule dynamin inhibitors that block endocytosis mediated by dynamin I or dynamin II. *Mol Pharmacol*. 2007; 72:1425–1439. [PubMed: 17702890]
23. Smirnova E, Shurland DL, Ryazantsev SN, van der Blik AM. A human dynamin-related protein controls the distribution of mitochondria. *J Cell Biol*. 1998; 143:351–358. [PubMed: 9786947]
24. Friedman JR, Lackner LL, West M, DiBenedetto JR, Nunnari J, Voeltz GK. ER tubules mark sites of mitochondrial division. *Science*. 2011; 334:358–362. [PubMed: 21885730]
25. Montessuit S, Somasekharan SP, Terrones O, Lucken-Ardjomande S, Herzig S, Schwarzenbacher R, Manstein DJ, Bossy-Wetzel E, Basanez G, Meda P, Martinou JC. Membrane remodeling induced by the dynamin-related protein Drp1 stimulates Bax oligomerization. *Cell*. 2010; 142:889–901. [PubMed: 20850011]
26. Chang CR, Blackstone C. Dynamic regulation of mitochondrial fission through modification of the dynamin-related protein Drp1. *Ann N Y Acad Sci*. 2010; 1201:34–39. [PubMed: 20649536]
27. Santel A, Frank S. Shaping mitochondria: The complex posttranslational regulation of the mitochondrial fission protein DRP1. *IUBMB Life*. 2008; 60:448–455. [PubMed: 18465792]
28. Zhao J, Liu T, Jin S, Wang X, Qu M, Uhlen P, Tomilin N, Shupliakov O, Lendahl U, Nister M. Human MIEF1 recruits Drp1 to mitochondrial outer membranes and promotes mitochondrial fusion rather than fission. *Embo J*. 2011; 30:2762–2778. [PubMed: 21701560]
29. Zhang B, Alysandratos KD, Angelidou A, Asadi S, Sismanopoulos N, Delivanis DA, Weng Z, Miniati A, Vasiadi M, Katsarou-Katsari A, Miao B, Leeman SE, Kalogeromitros D, Theoharides TC. Human mast cell degranulation and preformed TNF secretion require mitochondrial translocation to exocytosis sites: relevance to atopic dermatitis. *J Allergy Clin Immunol*. 2011; 127:1522–1531. e1528. [PubMed: 21453958]
30. Cassidy-Stone A, Chipuk JE, Ingerman E, Song C, Yoo C, Kuwana T, Kurth MJ, Shaw JT, Hinshaw JE, Green DR, Nunnari J. Chemical inhibition of the mitochondrial division dynamin reveals its role in Bax/Bak-dependent mitochondrial outer membrane permeabilization. *Dev Cell*. 2008; 14:193–204. [PubMed: 18267088]
31. Verstreken P, Ly CV, Venken KJ, Koh TW, Zhou Y, Bellen HJ. Synaptic mitochondria are critical for mobilization of reserve pool vesicles at *Drosophila* neuromuscular junctions. *Neuron*. 2005; 47:365–378. [PubMed: 16055061]
32. Carneiro L, Allard C, Guissard C, Fioramonti X, Turrel-Cuzin C, Bailbe D, Barreau C, Offer G, Nedelec E, Salin B, Rigoulet M, Belenguer P, Penicaud L, Leloup C. Importance of mitochondrial dynamin-related protein 1 in hypothalamic glucose sensitivity in rats. *Antioxid Redox Signal*. 2012; 17:433–444. [PubMed: 22229526]
33. Ong SB, Subrayan S, Lim SY, Yellon DM, Davidson SM, Hausenloy DJ. Inhibiting mitochondrial fission protects the heart against ischemia/reperfusion injury. *Circulation*. 2010; 121:2012–2022. [PubMed: 20421521]
34. Brooks C, Wei Q, Cho SG, Dong Z. Regulation of mitochondrial dynamics in acute kidney injury in cell culture and rodent models. *J Clin Invest*. 2009; 119:1275–1285. [PubMed: 19349686]
35. Park SW, Kim KY, Lindsey JD, Dai Y, Heo H, Nguyen DH, Ellisman MH, Weinreb RN, Ju WK. A selective inhibitor of drp1, mdivi-1, increases retinal ganglion cell survival in acute ischemic mouse retina. *Invest Ophthalmol Vis Sci*. 2011; 52:2837–2843. [PubMed: 21372007]

36. Vandendries ER, Hamilton JR, Coughlin SR, Furie B, Furie BC. Par4 is required for platelet thrombus propagation but not fibrin generation in a mouse model of thrombosis. *Proc Natl Acad Sci U S A*. 2007; 104:288–292. [PubMed: 17190826]
37. VerPlank, L.; Dockendorff, C.; Negri, J.; Perez, JR.; Dilks, J.; MacPherson, L.; Palmer, M.; Flaumenhaft, R.; Schreiber, SL. Chemical Genetic Analysis of Platelet Granule Secretion-Probe 2. Probe Reports from the NIH Molecular Libraries Program. 2011. <http://www.ncbi.nlm.nih.gov/books/NBK47352/>
38. Cui M, Tang X, Christian WV, Yoon Y, Tieu K. Perturbations in mitochondrial dynamics induced by human mutant PINK1 can be rescued by the mitochondrial division inhibitor mdivi-1. *J Biol Chem*. 2010; 285:11740–11752. [PubMed: 20164189]
39. Lackner LL, Nunnari J. Small molecule inhibitors of mitochondrial division: tools that translate basic biological research into medicine. *Chem Biol*. 2010; 17:578–583. [PubMed: 20609407]
40. Wiederkehr A, Wollheim CB. Mitochondrial signals drive insulin secretion in the pancreatic beta-cell. *Mol Cell Endocrinol*. 2012; 353:128–137. [PubMed: 21784130]
41. Keating DJ. Mitochondrial dysfunction, oxidative stress, regulation of exocytosis and their relevance to neurodegenerative diseases. *J Neurochem*. 2008; 104:298–305. [PubMed: 17961149]
42. Ye Y, Perez-Polo JR, Birnbaum Y. Protecting against ischemia-reperfusion injury: antiplatelet drugs, statins, and their potential interactions. *Ann N Y Acad Sci*. 2010; 1207:76–82. [PubMed: 20955429]
43. Hu H, Batteux F, Chereau C, Kavian N, Marut W, Gobeaux C, Borderie D, Dinh-Xuan AT, Weill B, Nicco C. Clopidogrel protects from cell apoptosis and oxidative damage in a mouse model of renal ischaemia-reperfusion injury. *J Pathol*. 2011; 225:265–275. [PubMed: 21630270]
44. Iwama D, Miyamoto K, Miyahara S, Tamura H, Tsujikawa A, Yamashiro K, Kiryu J, Yoshimura N. Neuroprotective effect of cilostazol against retinal ischemic damage via inhibition of leukocyte-endothelial cell interactions. *J Thromb Haemost*. 2007; 5:818–825. [PubMed: 17408412]

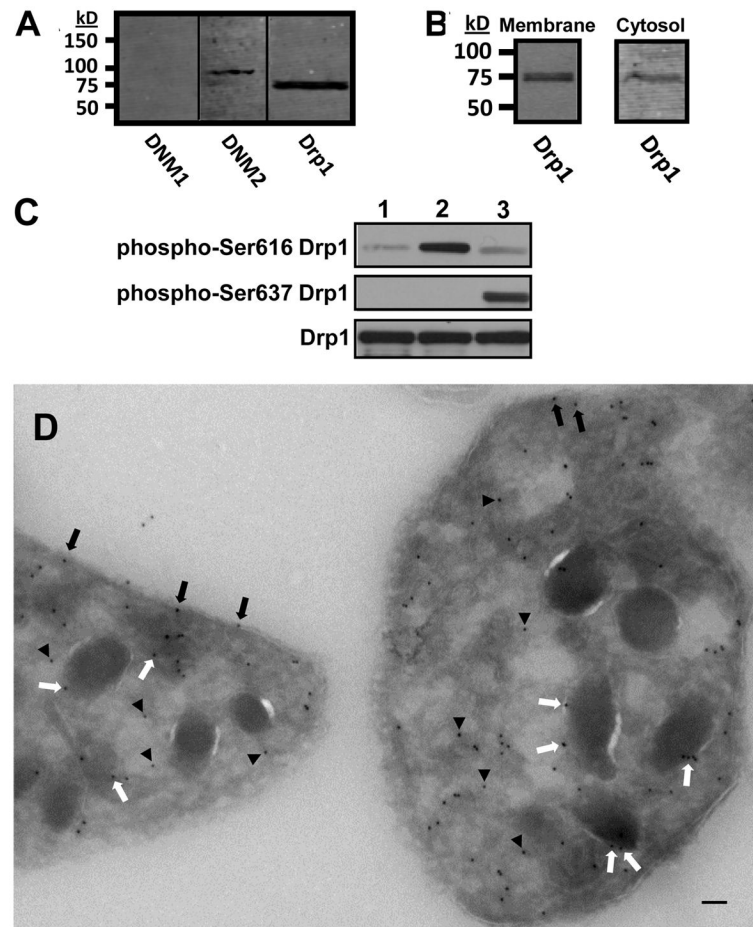


Figure 1. Detection and localization of Drp1 in platelets

(A) Human platelet lysates were evaluated for dynamin 1 (*DNMI*), dynamin 2 (*DNM2*), and dynamin-related protein-1 (*Drp1*) as indicated. (B) Platelet cytosol and membranes were evaluated for Drp1. (C) Platelets were incubated with either 1) buffer alone, 2) 5 μ M SFLLRN, or 3) 10 μ M forskolin. Lysates were then evaluated using either an anti-Ser616 Drp1 phosphorylation site specific antibody (*phospho-Ser616 Drp1*), an anti-Ser637 Drp1 phosphorylation site specific antibody (*phospho-Ser637 Drp1*), or an antibody to detect total Drp1 (*Drp1*). (D) Immunogold staining of resting platelets demonstrates Drp1 associated with plasma membrane (*black arrows*), granule membranes (*white arrows*), and cytosol (*black arrowheads*). Scale bar, 100 nm.

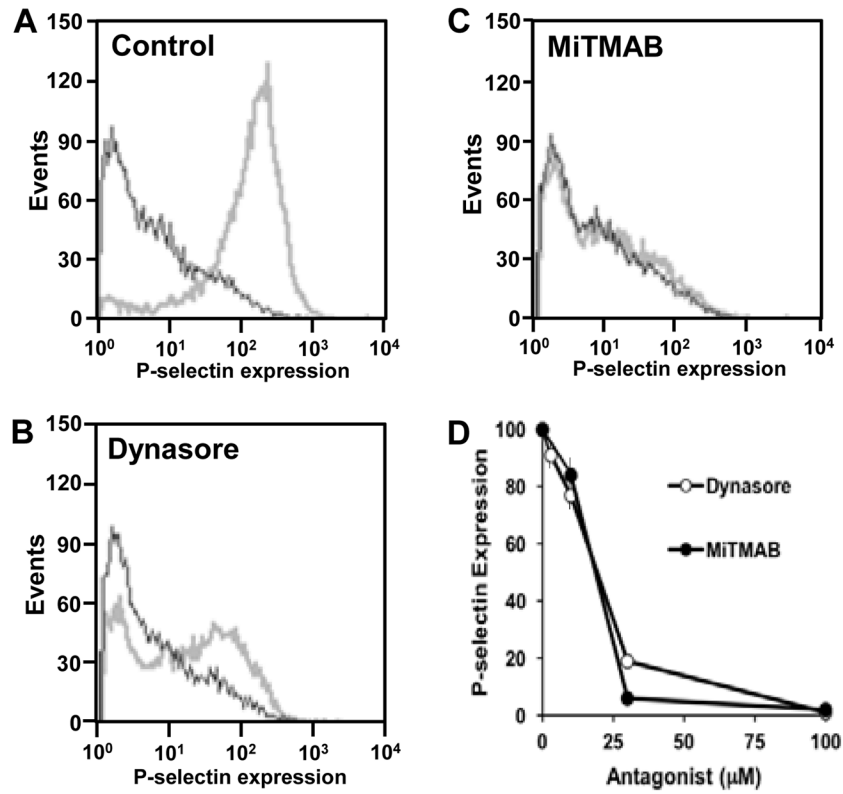


Figure 2. Inhibition of dynamin blocks α -granule secretion.

Human platelets were incubated in the presence of either (A) vehicle alone, (B) dynasore, or (C) MiTMAB and subsequently exposed to buffer (*black*) or 5 μ M SFLLRN (*gray*). P-selectin surface expression was subsequently evaluated by flow cytometry. (D) Both dynasore and MiTMAB inhibited PAR1-mediated P-selectin expression in a dose-dependent manner ($n = 3 \pm$ S.D.).

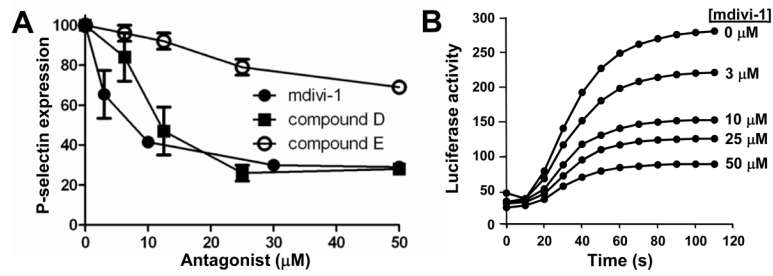


Figure 3. Role of Drp1 in α -granule and dense granule exocytosis.

(A) Platelet P-selectin surface expression in response to 5 μM SFLLRN was assayed in the presence of the indicated concentrations of either mdivi-1 (*black circle*), compound D (*black square*) or compound E (*open circle*). Data are representative of 3 experiments \pm S.D. (B) Platelets were incubated with the indicated concentrations of mdivi-1 for 20 minutes prior to addition of 5 μM SFLLRN. Release of adenine nucleosides was subsequently monitored using a luciferin-luciferase assay. Data are representative of 3 similar experiments.

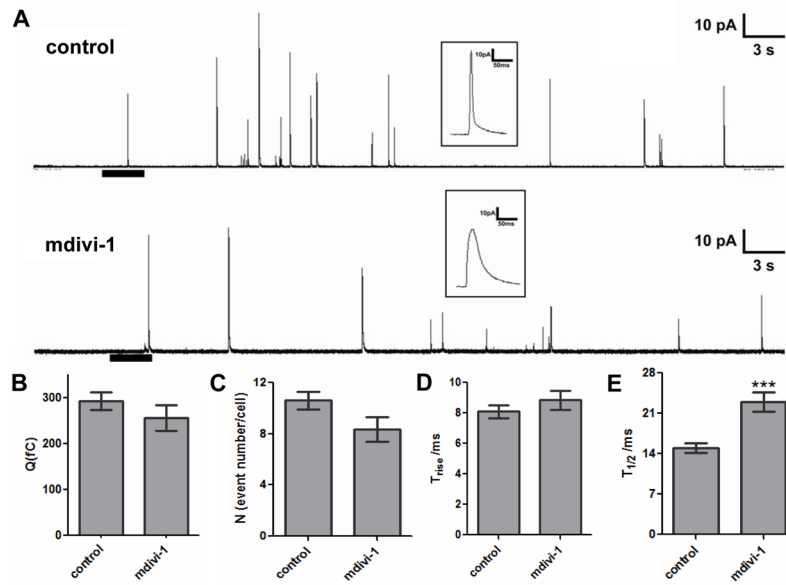


Figure 4. Role of Drp1 in the kinetics of platelet granule release

(A) Representative amperometric traces of rabbit platelet dense granule release in the presence and absence of mdivi-1. The heavy bar beneath the tracings indicates the time and the duration of the thrombin stimulation. *Insets*: The distinct spike shapes for control (*upper*) and mdivi-1 (*lower*) conditions depicted in the millisecond time scale demonstrate different serotonin release kinetics. Mdivi-1 (10 μ M) did not influence quantal release (B), the number of granules released per cell (C), or the time required for transition from fusion pore to full fusion (T_{rise}) (D). However, the total time required for the release event ($T_{1/2}$) was longer for platelets exposed to mdivi-1 ($p < 0.001$) (E). Data represent the average \pm S.E.M. of 107 control tracings and 39 tracings from platelets exposed to mdivi-1.

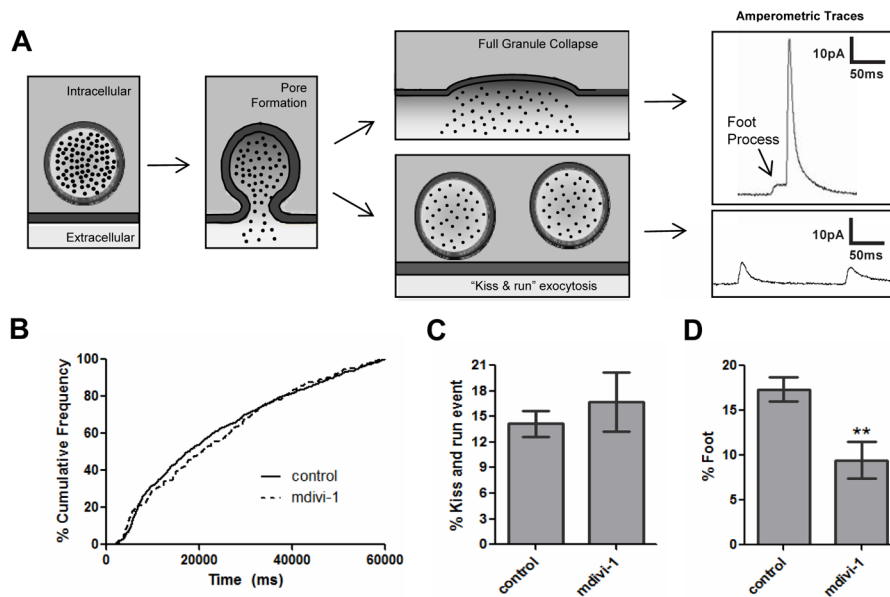


Figure 5. Role of Drp1 in stability of the platelet fusion pore

(A) During platelet granule exocytosis, a fusion pore forms as indicated by the foot process, shown as the initial inflection in the top amperometric tracing. This pore can then dilate rapidly, resulting in full granule collapse and complete release of granule contents as indicated by the spike (*upper amperometric tracing*). Alternatively, the fusion pore may reseal in a kiss-and-run event. This phenomenon typically results in a shallow inflection in the current tracing representing the release of a small amount of serotonin (*lower amperometric tracing*). (B) Cumulative frequency analysis in the presence and absence of 10 μ M mdivi-1 demonstrated no difference in the rate of rabbit platelet dense granule release. Amperometric spikes were evaluated to determine (C) the percentage of kiss-and-run events and (D) the percent of spikes preceded by a foot process in the presence and absence of mdivi-1. These results demonstrate that mdivi-1 interferes with the expansion of the fusion pore to full fusion through a foot process, as indicated by the significant difference between the %foot values for mdivi-1-treated and control platelets ($p < 0.01$). Data represent the average \pm S.E.M. of 107 control tracings and 39 tracings from platelets exposed to mdivi-1.

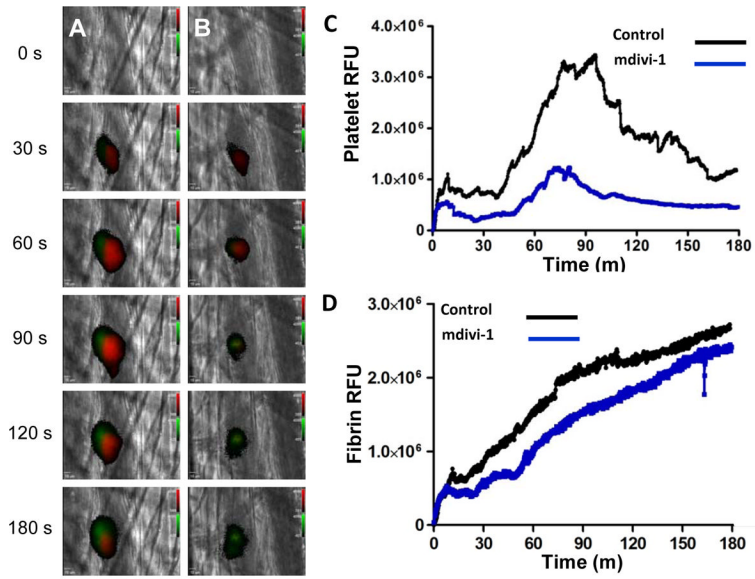


Figure 6. Effect of mdivi-1 on platelet accumulation and fibrin generation during thrombus formation following laser injury of cremaster arterioles

Mouse platelet-specific anti-CD42b antibody conjugated to Dylight 649 (0.1 $\mu\text{g/g}$ body weight) and fibrin-specific mouse anti-human fibrin II β -chain monoclonal antibody conjugated to Alexa 488 (0.5 $\mu\text{g/g}$ body weight) were infused into the mouse. Mdivi-1 (50 mg/kg) was subsequently infused intravenously 5 minutes prior to the initial laser injury. Representative binarized images of the appearance of fluorescence signals associated with platelets (*red*) and fibrin (*green*) over 180 seconds following laser-induced vessel wall injury in a wild type mouse are shown in panels (A) vehicle alone and (B) 50 mg/kg mdivi-1. (C) Median integrated platelet fluorescence intensity and (D) median integrated fibrin fluorescence intensity at the injury site are plotted versus time. Data are from 28 thrombi in 3 mice for control condition and 24 thrombi in 3 mice for mdivi-1 condition.